Abdominal Radiology (2020) 45:982–1000
https://doi.org/10.1007/s00261-019-02082-4

SPECIAL SECTION: ADRENAL GLAND

Mimics, pitfalls, and misdiagnoses of adrenal masses on CT and MRI

Khaled M. Elsayes[1] · Mohab M. Elmohr[1] · Sanaz Javadi[1] · Christine O. Menias[2] · Erick M. Remer[3] · Ajaykumar C. Morani[1] · Akram M. Shaaban[4]

Published online: 4 June 2019

Abstract
Due to the widespread use of imaging, incidental adrenal masses are commonly encountered. A number of pitfalls can result in misdiagnosis of these lesions, including inappropriate choice of imaging technique, presence of pseudolesions, and overlap of imaging features of different adrenal lesions. This article explores the potential pitfalls in imaging of the adrenal glands, on computed tomography and magnetic resonance imaging, that can lead to misinterpretation. Clues to correct diagnoses are provided to evade potential misinterpretation.

Keywords Adrenal gland · CT · MRI · Mimics

Introduction

Incidental adrenal masses are a relatively common finding on cross-sectional imaging. An adrenal incidentaloma is an adrenal mass measuring 1 cm or larger discovered on an imaging examination that has been obtained for an unrelated indication [1]. The prevalence of adrenal incidentalomas on computed tomography (CT) is estimated to be 4.2% [2]. The vast majority of adrenal incidentalomas are benign, with non-functioning adrenocortical adenomas (ACAs) representing approximately 75% of all incidentalomas [3, 4]. Unlike incidentalomas, adrenal malignancies are not common and typically follow an aggressive course with rapid growth and metastases [5]. A wide spectrum of other pathologies can occur in the adrenal gland, leading to a relatively long list of differential diagnoses. In addition, several pseudolesions can falsely mimic an adrenal lesion on imaging.

In this article, we review imaging features of pitfalls and mimics that are related to various abnormalities within or adjacent to the adrenal glands and can potentially lead to erroneous diagnosis. We also provide clues to help reach a specific diagnosis and avoid potential misinterpretation of these entities.

Pitfalls related to imaging technique

Dedicated adrenal washout protocol typically comprises three phases acquired at specific times in relation to intravenous contrast administration for CT of the adrenal gland. The unenhanced phase is obtained prior to contrast administration, while the early and delayed enhanced phases are obtained at 60–80 s and 15 min, respectively, after contrast administration. Suboptimal imaging technique can result in misdiagnosis of adrenal masses [6].

Suboptimal delayed phase

The precise timing of contrast administration and image acquisition is crucial for the characterization of adrenal lesions relying on their typical contrast enhancement and washout patterns. For example, ACA demonstrates characteristic rapid contrast enhancement followed by rapid washout [7]. A dedicated adrenal CT protocol allows for the calculation of washout percentages, especially absolute percentage washout (APW); APW ≥ 60% is highly sensitive for ACA, with a reported range of 96–100% [8–10].

✉ Khaled M. Elsayes
kmelsayes@mdanderson.org

[1] Department of Diagnostic Radiology, The University of Texas MD Anderson Cancer Center, Houston, TX 77030, USA

[2] Department of Radiology, Mayo Clinic, Scottsdale, AZ, USA

[3] Imaging Institute, Cleveland Clinic, Cleveland, OH, USA

[4] Department of Diagnostic Radiology, University of Utah, Salt Lake City, UT, USA

$$\text{APW} = \frac{\text{Early Attenuation Value} - \text{Delayed Attenuation Value}}{\text{Early Attenuation Value} - \text{Unenhanced Attenuation Value}} \times 100$$

Care should be taken, when calculating washout percentages, that the delayed scans are acquired 15 min after intravenous contrast administration. Although early image acquisition is more convenient for both the patient and the imaging facility, it results in a significant decrease in diagnostic sensitivity, from 96–100 to 55–79%, depending on the threshold used (Fig. 1) [8, 11, 12]. A recent study showed no diagnostic advantage in acquiring 10-min-delayed contrast-enhanced images over non-enhanced CT images [6]. This finding can be attributed to insufficient time for the washout of the adrenal lesion to adequately manifest; resulting in potentially higher attenuation values on delayed images and lower washout percentages [13]. Another recent study showed that early enhanced CT (~ 70 s postcontrast) in combination with quantitative CT image features could be used to accurately characterize adrenal lesions as benign or malignant without the need for delayed images; however, this approach is still under investigation and has not been implemented clinically [14]. In summary, a suboptimal delayed phase could fail to confirm the diagnosis of an ACA.

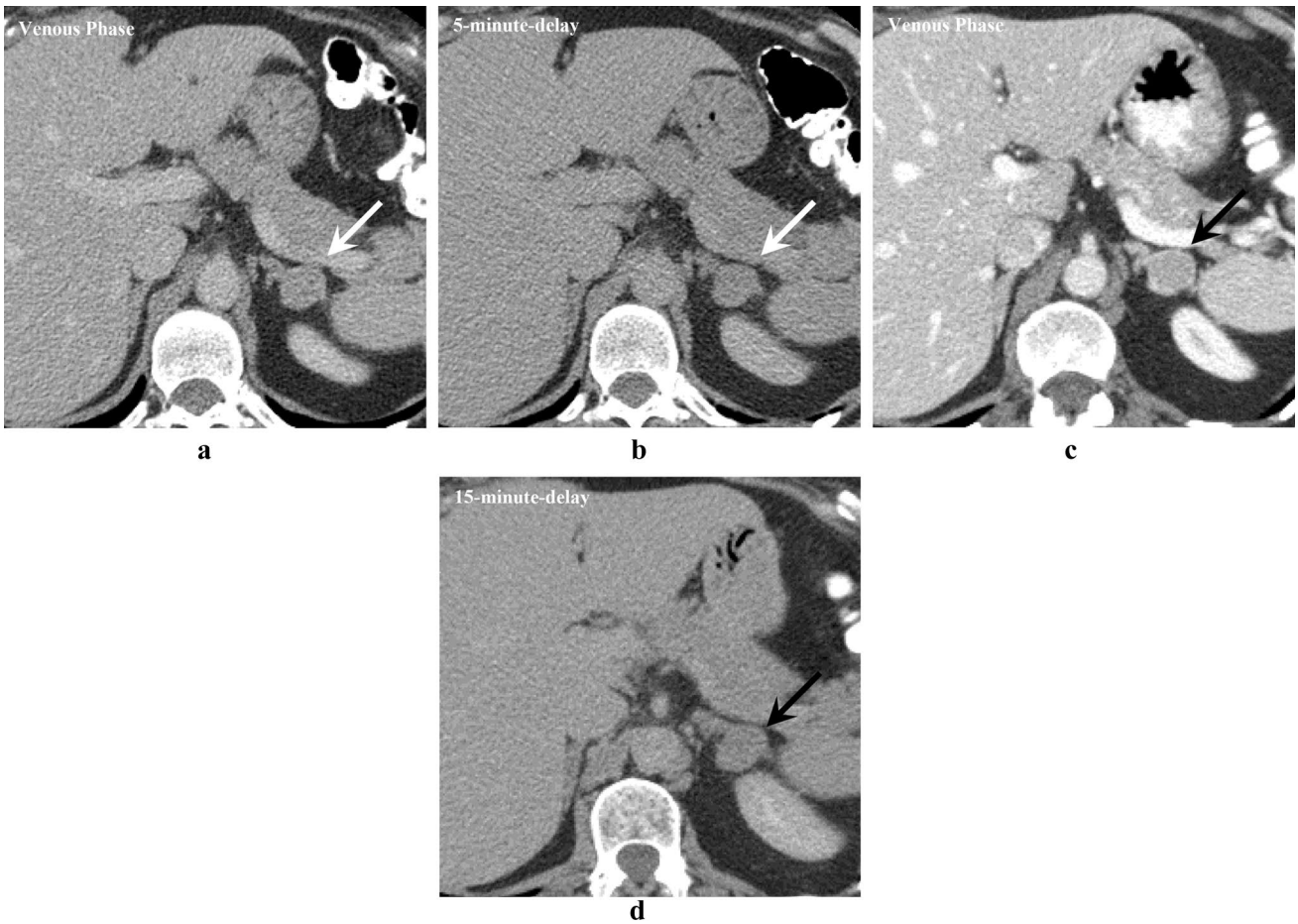

Fig. 1 An example of suboptimal delay time in a 60-year-old woman with left adrenocortical adenoma. Contrast-enhanced axial CT **a** and **b** shows an oval-shaped nodule (arrow) within the left adrenal gland with precontrast (not shown) attenuation of 45 HU, venous phase **a** attenuation of 75 HU, 5-min-delayed phase **b** attenuation of 61 HU, and absolute washout of 47%, which is not typical for adrenal adenoma. Contrast-enhanced axial CT **c** and **d** was repeated with an optimal 15-min delay and again showed the left adrenal nodule with precontrast (not shown) attenuation of 41 HU, venous phase **c** attenuation of 115 HU, 15-min-delayed phase **d** attenuation of 54 HU, and absolute washout of 82%, which is consistent with adrenal adenoma; the lesion was later resected and confirmed to be an adrenocortical adenoma. This case illustrates an important pitfall as the nodule was considered indeterminate based on suboptimal delay time

Key point

– A dedicated adrenal CT protocol with 15-min delay should be used when calculating washout percentages for adrenal masses. *Suboptimal delay can lead to erroneous diagnosis.*

Pitfalls related to the utility of CT and MRI

Understanding the utility of the various imaging modalities and their limitations is important in accurately characterizing adrenal lesions. Various imaging modalities exist for imaging the adrenal glands, including CT, magnetic resonance imaging (MRI), and positron emission tomography (PET)/CT.

CT, because of its low cost and high accuracy, is recommended as the initial imaging modality for evaluating an incidental adrenal mass [15, 16]. Unenhanced CT readily identifies ACA, as most ACAs have low attenuation due to their abundant intracellular lipid content [17]. By using a threshold of 10 Hounsfield units (HU), unenhanced CT achieved a sensitivity ranging from 40 to 70% and a specificity ranging from 98 to 100% in distinguishing lipid-rich adenomas [17, 18]. No further testing is required if the adrenal mass is < 10 HU with imaging features suggesting benignity (e.g., homogeneity, well-defined borders, stability over time). Approximately 30% of adenomas are lipid poor which demonstrate attenuation values > 10 HU. Lipid-poor adenomas exhibit characteristic enhancement and washout patterns that can be exploited on adrenal CT protocol, as discussed previously.

MRI also has the ability to differentiate adrenal adenomas from non-adenomas based on their inherent tissue characteristics [19]. Chemical shift MRI (CSI) is particularly useful in the diagnosis of adenomas because of its characteristic loss of signal intensity on out-of-phase (OP) compared to in-phase (IP) images based on the difference in precession frequency of water and fat molecules [7, 20]. The percentage of signal loss is referred to as the adrenal signal intensity index (ASII); an ASII of > 16.5% on 1.5 Tesla (T) MR scanners is diagnostic of adrenal adenomas [21]. $\text{ASII} = \frac{(\text{lesion IP})-(\text{lesion OP})}{(\text{lesion IP})} \times 100$. Studies have shown the ability of CSI to characterize 89% of adenomas with attenuations of 10–30 HU on unenhanced CT [22]. However, 8% of ACAs do not demonstrate loss of signal intensity on CSI, due to their insufficient intracellular lipid content (Fig. 2) [23–25]. This has been proven to be a limitation of CSI and could be problematic, especially in ACAs with precontrast CT attenuation > 30 HU [22, 24].

A potential pitfall when evaluating an adrenal mass on MRI is calculating the washout percentages based on their signal intensity on the precontrast and contrast-enhanced phases. To our knowledge, studies for adapting washout thresholds for MRI have been limited and had conflicting results [21]. Therefore, the calculation of washout percentages for diagnosis of adrenal adenomas should be limited to CT with adrenal protocol.

During the interpretation of an imaging study of the adrenal glands, care should be taken that scan parameters were kept the same among all phases of CT or MRI. Scan parameters, including both acquisition and reconstruction parameters, can potentially affect attenuation values and lead to misinterpretation of the imaging study.

Key points

– An adrenal mass with precontrast attenuation of < 10 HU on CT is diagnostic for lipid-rich adenoma and obviates the need for washout study.
– On MRI, significant drop of signal intensity on OP compared to IP images is diagnostic for adrenal adenoma.
– Calculation of washout should be limited to contrast-enhanced CT with adrenal protocol.
– Scan parameters should be the same among different phases.

Inaccurate placement of the region of interest

A common pitfall that can occur when evaluating a CT or MRI study is the inaccurate placement of the region of interest (ROI) for calculation of attenuation values. It is essential to place the ROI tool to cover at least one-half to two-thirds of the adrenal mass, excluding any necrotic area, when applicable [26]. It should also be noted that the ROI is to be placed over a homogeneous region for accurate measurement. Incorrect placement can lead to the underestimation or overestimation of the attenuation values.

Key point

– The ROI should cover one-half to two-thirds of the adrenal mass and be placed over a homogeneous region of the mass, excluding any necrotic areas.

Pitfalls related to anatomy

The adrenal glands are inverted Y-shaped organs with a body and two limbs: a medial limb and a lateral limb [27]. The adrenal glands are located in the retroperitoneum, anteromedially and superiorly to the kidneys. The right adrenal gland is adjacent to the right lobe of the liver, crus of the right hemidiaphragm, duodenum, inferior vena cava, and right kidney; whereas the left adrenal gland is adjacent to the spleen, pancreatic tail, stomach, and left kidney [28].

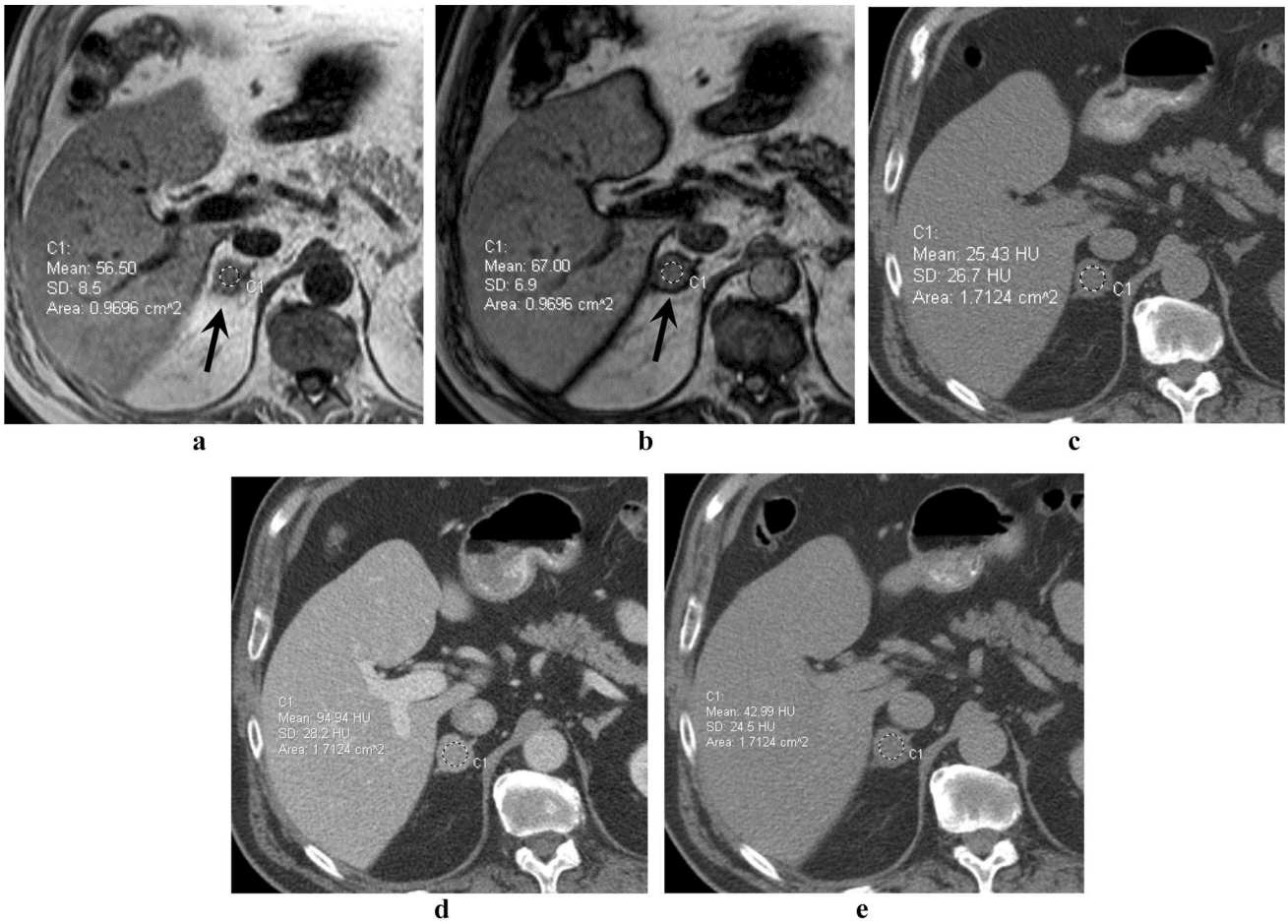

Fig. 2 An example of a lipid-poor adrenocortical adenoma without signal loss on opposed-phase compared to in-phase MR images in a 26-year-old man. T1-weighted axial MRI shows a round-shaped nodule (arrow) measuring 2.5 cm involving the right adrenal gland with no drop in signal intensity on out-of-phase **b** compared to in-phase **a** pulse sequences. Contrast-enhanced CT was performed 1 month later and demonstrated the same nodule with precontrast **c** attenuation of 25 HU, venous phase **d** attenuation of 95 HU, 15-min-delayed phase **e** attenuation of 43 HU, and absolute percentage washout of 74%, which is consistent with an adrenocortical adenoma. The adrenal mass was surgically resected and proven to be an adrenocortical adenoma. Caution should be exercised when evaluating lipid-poor adenomas on MRI, as 8% of lipid-poor adenomas do not show signal loss on out-of-phase compared to in-phase pulse sequences

Masses arising from adjacent structures can potentially be mistaken for adrenal lesions. Multiplanar reformats can help distinguish the adrenal glands from adjacent structures and allow the vast majority of these lesions to be distinguished from true adrenal lesions.

Adrenal pseudonodule

In some instances, a completely normal adrenal gland can be misidentified as a pathological adrenal nodule; such misidentification can be attributed to the gland's appearance when viewed on a single plane, most commonly the axial plane. Due to the normal variations in the shape, orientation, and location of the adrenal glands, a horizontally oriented limb of the adrenal gland can mimic an adrenal nodule in the axial plane. However, upon examination of the multiplanar reformatted (MPR) images in the coronal and sagittal planes, the normal adrenal gland can be clearly identified (Fig. 3). Likewise, a vertically oriented limb can be easily recognized in the axial plane, but it may mimic an adrenal nodule on the coronal plane. Therefore, it is useful to make use of MPR on CT or alternate imaging planes on MRI to confirm suspected nodules.

Exophytic gastric lesions

Gastric diverticula are rare outpouchings of the gastric wall that commonly arise from the gastric fundus, with a prevalence of 0.02% in autopsies and 0.04% on upper gastrointestinal series [29]. Gastric discomfort and post-prandial fullness are unusual manifestations, as symptomatic gastric diverticula are rare and are most often discovered

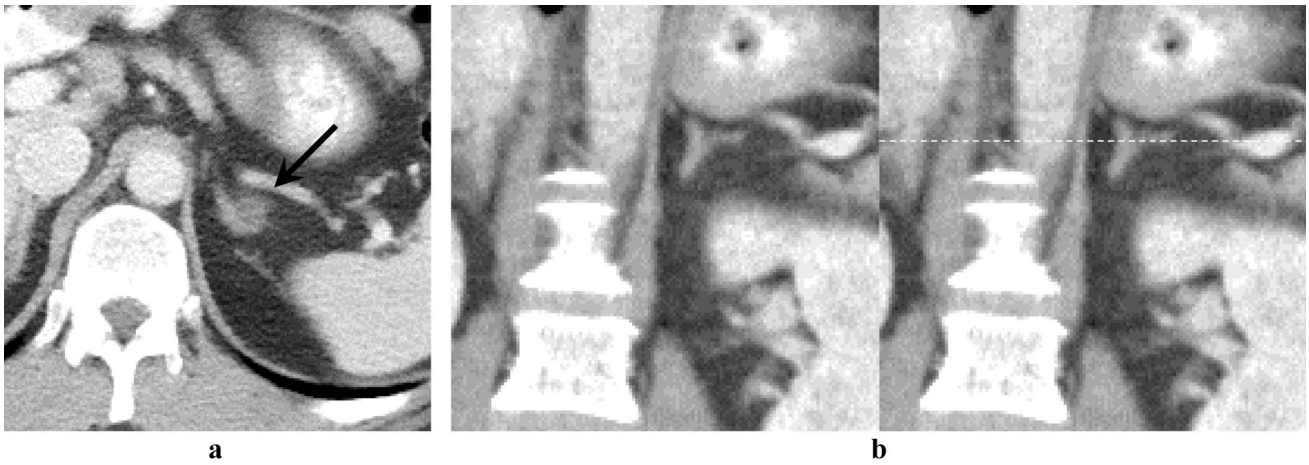

Fig. 3 An adrenal pseudonodule in a 24-year-old woman with hyperparathyroidism. Contrast-enhanced axial CT **a** shows an oval structure (arrow) in the left suprarenal region that was suspected to be an adrenal nodule. However, coronal reformatted images **b** did not show the structure, and a normal left adrenal gland was noted

Fig. 4 An example of gastric diverticulum mimicking an adrenal nodule in a 69-year-old man. Contrast-enhanced axial CT **a** shows a hypoattenuating nodule (arrow) in the left suprarenal region that was suspected to be a left adrenal nodule. Follow-up intravenous and oral contrast-enhanced axial CT **b** shows the communication (black arrow) between the structure (white arrow) and the gastric fundus, with layering of the oral contrast material within the gastric diverticulum

incidentally [30, 31]. Occasionally, a gastric fundal diverticulum (Fig. 4) can be misinterpreted as a left adrenal mass, especially when filled with fluid [32]. MPR images can be helpful in such cases, especially with oral contrast, to visualize the communication between the gastric cavity and the diverticulum. A key finding, in such cases, is the identification of gas within the suspected lesion (gas may not be present or can be very minimal in amount). On MRI, the presence of gas inside the diverticulum can cause susceptibility artifacts.

Other exophytic gastric lesions that are adjacent to the adrenal glands, including gastrointestinal stromal tumors, can potentially be mistaken for adrenal lesions [33].

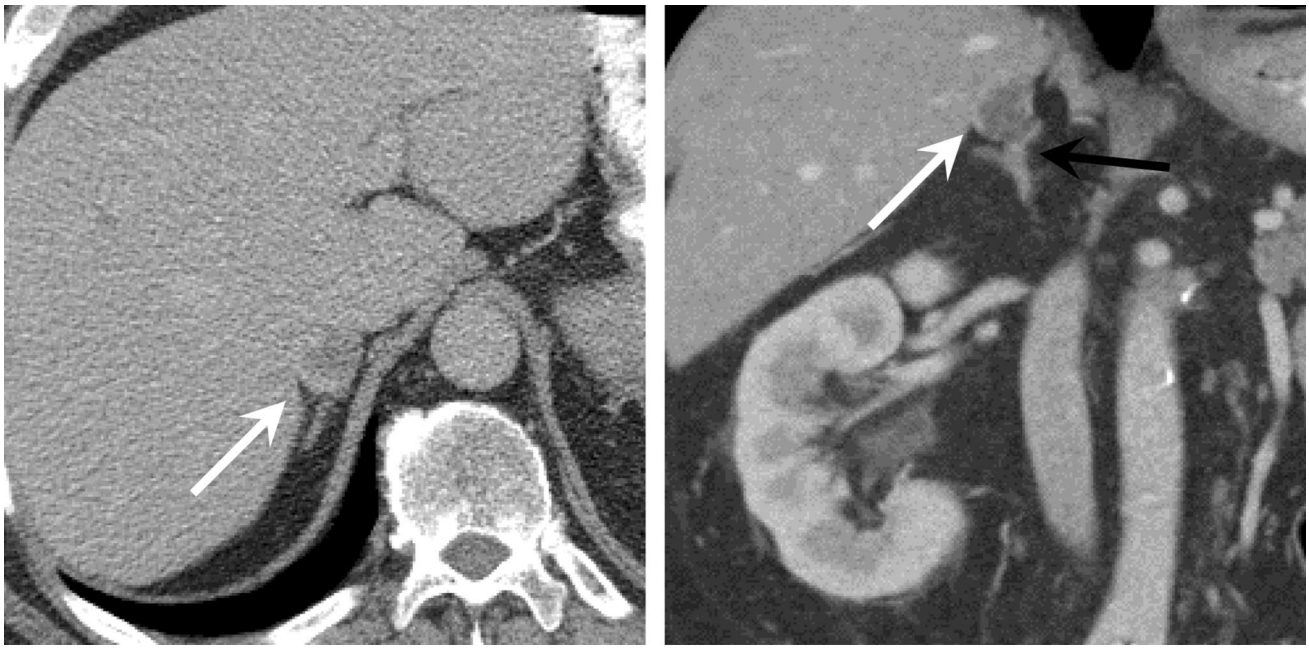

Fig. 5 An example of an exophytic hepatic mass mimicking an adrenal nodule in a 50-year-old man with hepatic hemangioma. Contrast-enhanced axial CT **a** in the delayed phase shows a hypoattenuating nodule (arrow) in the right suprarenal region suspected to be a right adrenal nodule. However, coronal reformation **b** shows the lesion (white arrow) to be arising from the right hepatic lobe. The right adrenal gland (black arrow) is seen separate from the lesion

Exophytic hepatic lesions

Occasionally, exophytic hepatic lesions can appear inseparable from the right adrenal gland and may pose a diagnostic challenge due to unclear origin [34, 35]. Hemangioma is the most common benign mesenchymal tumor of the liver. Pedunculated hemangiomas represent 12% of hepatic hemangiomas and tend to be larger in size [36, 37]. Typical imaging features of hemangiomas are diagnostic, and MPR is helpful in detecting a mass attached to the liver and identifying the adrenal gland separate from the exophytic hepatic lesion (Fig. 5).

Pitfalls related to adjacent vascular structures

Extrahepatic portosystemic shunts in the setting of portal hypertension may give rise to several collaterals or varices in the upper abdomen. For example, the inferior phrenic vein, which runs immediately anterior to the adrenal gland, connects the splenic vein (portal system) to the left renal vein (systemic) and can result in adrenal or periadrenal varices [38, 39]. A periadrenal varix could be interpreted as an adrenal tumor, and an attempted excision or biopsy could be catastrophic. On CT, early intense enhancement is not uncommon; the left inferior phrenic vein can be seen draining into the left renal vein on MPR

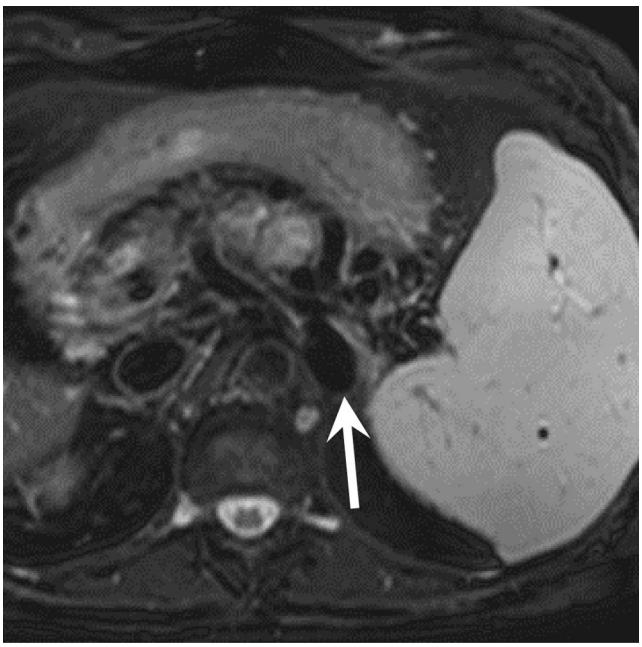

Fig. 6 An example of a vascular structure mimicking an adrenal nodule in a 67-year-old man with hepatocellular carcinoma. Axial T2-weighted MRI shows an enlarged retroperitoneal collateral (arrow) in the expected location of the left adrenal gland with a flow void consistent with a vessel. The left adrenal gland cannot be definitely visualized

images [39, 40]. While on MRI, vascular structures tend to exhibit the flow void phenomenon, appearing as loss of signal on spin-echo techniques (Fig. 6). It should be noted, however, that flow void is dependent upon vascular patency and blood flowing at a sufficient velocity [41].

Other vascular structures, including venous and arterial aneurysms and pseudoaneurysms, abutting the adrenal glands are rare but can be potentially mistaken for adrenal lesions [42].

Splenules and splenosis

Ectopic splenic tissue (EST) is a benign incidental finding seen in up to 16% of abdominal CT examinations [43]. Splenules (*accessory spleens, or splenunculi*) represent a congenital subtype of ectopic normal splenic tissue that occurs as a result of failure of fusion during embryogenesis [43], whereas splenosis represents the acquired form of EST seen after trauma or surgery. EST can be located almost anywhere in the abdomen—usually near the splenic hilum—with the exception of splenosis, which can also be located in the thorax [44]. EST situated in the suprarenal region has been reported to mimic adrenal masses (Fig. 7) [45, 46]. ESTs typically appear as well-marginated, round nodules exhibiting the same density/intensity and enhancement characteristics of the spleen. Diagnosis can be confirmed with technetium 99 m (Tc 99 m) sulfur colloid scintigraphy, which demonstrates high uptake in the splenic tissue [43]. However, Tc 99 m heat-denatured red blood cell scintigraphy, with its greater specificity, remains the gold standard for detecting splenic tissue [47]. It is worth noting that the addition of single-photon emission CT and CT (SPECT/CT) to either of the previously mentioned nuclear scans significantly improves sensitivity [48]. The diagnosis of EST should be excluded, using the appropriate imaging modalities and clinical correlation (i.e., history of abdominal trauma, or splenic rupture), when evaluating a suprarenal mass with suspicious imaging features.

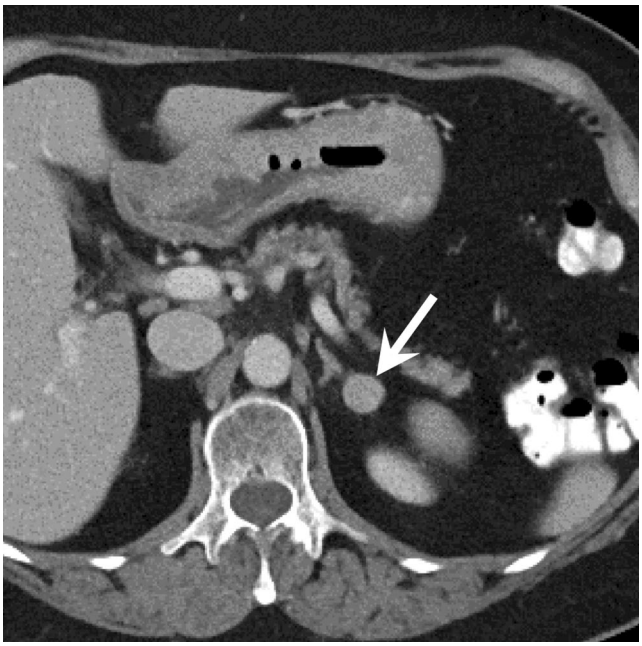

Fig. 7 An example of a splenule mimicking a left adrenal mass. Contrast-enhanced axial CT shows a well-circumscribed, round 1.6-cm nodule (arrow) in the left suprarenal region. Relative washout was 42.5% (no precontrast images were available for calculation of the APW), which is consistent with an adrenocortical adenoma. However, biopsy confirmed the diagnosis of a splenule

Celiac ganglion

The celiac ganglia are the largest of the autonomic celiac plexus, innervating most of the gastrointestinal tract. They are located in the upper abdomen, with one on each side of the aorta and medial to the adrenal glands [49]. The celiac ganglia measure approximately 0.5 cm in diameter, and the left ganglion is usually visualized more than the right ganglion (89% vs 67%) [50]. This structure can be potentially misinterpreted for an adrenal mass, given its location and morphology. The celiac ganglia are multilobular or, less commonly, discoid in shape [51]. On CT, soft-tissue attenuation is seen, similar to adenomas, in the unenhanced and early enhanced phases; however, in the delayed phase, celiac ganglia typically exhibit progressive enhancement [50]. Evaluation on MPR allows the recognition of a celiac ganglion as a separate structure from the adrenal gland (Fig. 8).

Key point

– Thorough evaluation of the sagittal and coronal planes is crucial in avoiding pitfalls related to adjacent anatomical structures or pathologies.

Mimics of adrenal adenoma

Simple adrenal cyst

Adrenal cysts are uncommon, with a prevalence estimated from 0.064 to 0.18% and constituting around 5.7% of adrenal incidentalomas [52, 53]. They are three times more common in women than in men and tend to be unilateral, occurring with equal frequency on each side. Adrenal cysts are usually discovered incidentally but can present with abdominal pain, hemorrhage, or cyst rupture. They are classified into four histological subtypes, in decreasing order of incidence: endothelial cysts, pseudocysts, epithelial cysts, and parasitic cysts. Endothelial cysts are the most common subtype,

a **b**

Fig. 8 An example of celiac ganglion mimicking an adrenal nodule in a 38-year-old woman with lung cancer. Contrast-enhanced axial CT **a** shows a sub-centimeter nodule (arrow) in the left suprarenal region suspected to be an adrenal adenoma. Coronal reformatting **b** shows the nodule (arrow) separate from the left adrenal gland and revealed it as the left celiac ganglion

Fig. 9 An example of a simple adrenal cyst mimicking an adrenal adenoma in a 54-year-old woman. Precontrast axial CT shows a nodule (arrow) that was suspected to be an adrenal lipid-rich adenoma within the left adrenal gland with attenuation of 6 HU. The nodule was found to demonstrate no enhancement on postcontrast CT with a thin, imperceptible wall, and markedly increased signal intensity on T2-weighted MRI, consistent with a simple cyst

accounting for nearly 45% of all adrenal cysts. Uncomplicated adrenal cysts demonstrate typical imaging features. However, because they are filled with fluid, they show low attenuation on unenhanced CT ≤ 20 HU. Therefore, an adrenal cyst can mimic a lipid-rich adenoma if its attenuation value is < 10 HU. Adrenal cysts lack the characteristic postcontrast enhancement of ACAs (Fig. 9) [54, 55]. MRI easily confirms an adrenal cyst, with marked hyperintensity on T2-weighted sequences and lack of signal loss on opposed-phase gradient echo T1-weighted images.

Key points

- Simple adrenal cysts show fluid attenuation on precontrast CT and thus can mimic lipid-rich adenomas on unenhanced CT.
- Lack of postcontrast enhancement and markedly increased signal intensity on T2-weighted MRI are characteristics of simple cysts.

Adrenal metastases containing intracellular lipid

The most common malignant lesions involving the adrenal gland are metastases. In fact, the adrenal gland is a common site for metastases, which are seen in up to 27% of autopsies of patients with known primary malignancies [56]. Tumors

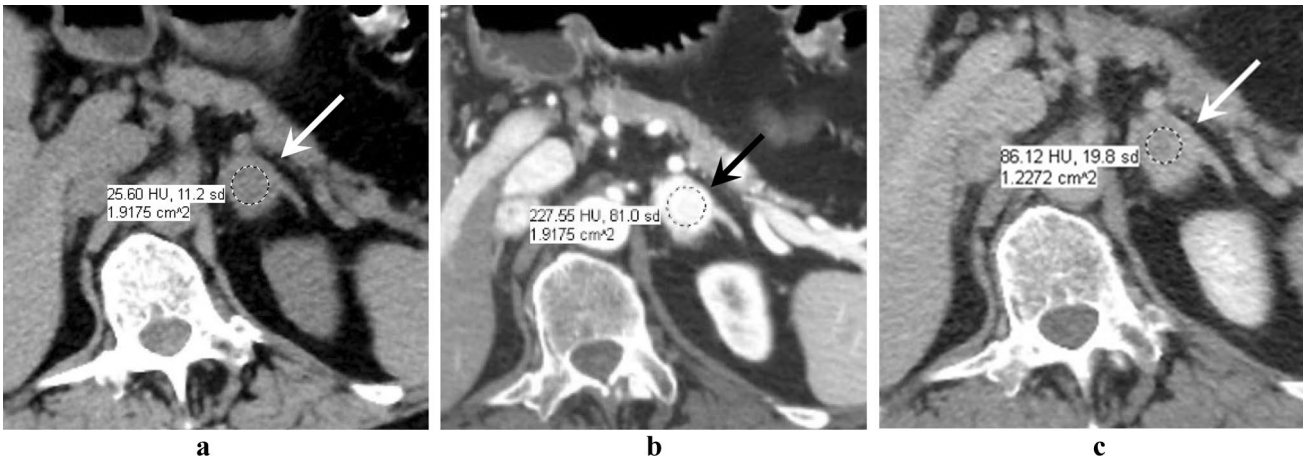

Fig. 10 An example of adrenal metastasis demonstrating washout in a 67-year-old man with clear cell renal cell carcinoma. Contrast-enhanced axial CT shows an oval-shaped nodule (arrow) within the left adrenal gland with precontrast **a** attenuation of 26 HU, venous phase **b** attenuation of 228 HU, 15-min-delayed phase **c** attenuation of 86 HU, and absolute washout of 70%, which is typical of adrenocortical adenoma. However, the high attenuation on the venous phase (228 HU) is not consistent with adrenocortical adenoma. The mass was later resected and proven to be an adrenal metastasis from clear cell renal cell carcinoma

known to metastasize to the adrenal glands include breast cancer, lung cancer, colorectal cancer, pancreatic cancer, renal cell carcinoma, melanoma, and hepatocellular carcinoma [57]. Adrenal metastases are usually solitary and asymptomatic, with a variable CT appearance and sluggish washout of contrast. Metastases from clear cell renal cell carcinoma (CRCC) and hepatocellular carcinoma (HCC) may contain an abundant amount of intracellular lipid and can, thereby, demonstrate low attenuation on non-contrast CT [58]. On contrast-enhanced CT, APW of more than 60% can be seen, mimicking adrenal adenomas (Fig. 10) [58]. A drop of signal intensity on OP compared to IP pulse sequences can be seen on MRI, mimicking adenoma.

Although lipid-rich metastases exhibit washout characteristics similar to adrenal adenomas, an attenuation of > 140 HU in the venous phase should raise the suspicion of vascular metastases such as CRCC or HCC [58]. Ancillary imaging features favoring metastases include local invasion, cystic changes, necrosis, and hemorrhage [59]. Positron emission tomography (PET)/CT can show avid FDG uptake by the metastatic deposits, and is highly sensitive and specific in this regard, when the lesion in question has a standardized uptake value (SUV) of > 3.1 [60, 61].

Key points

- Adrenal metastasis from HCC and CRCC can demonstrate washout characteristics similar to ACA.
- Venous phase attenuation of > 140 HU should raise suspicion of vascular metastases.
- Metastases containing intracellular lipid (such as those from HCC and CRCC) can demonstrate signal drop on OP compared with IP pulse MRI sequences, thus mimicking adenoma.
- Avid FDG uptake on PET/CT can help confirm the diagnosis of metastasis.

Pheochromocytoma demonstrating washout

Pheochromocytomas are rare catecholamine-secreting neuroendocrine tumors arising from the chromaffin cells, mostly of the adrenal medulla, with a reported incidence of 0.05% [62]. Asymptomatic pheochromocytoma is increasingly diagnosed as an incidental adrenal mass [63]. It typically appears on CT as a heterogeneously enhancing mass ranging in size from 4 to 6 cm [64, 65]. Pheochromocytomas show inconsistent washout patterns on adrenal CT protocol; up to one-third of pheochromocytomas demonstrate washout characteristics similar to ACA on delayed CT scans, and hence could be confused with adenomas [66–68].

A valuable clue to differentiating pheochromocytoma from adenoma on enhanced CT is the characteristic intense enhancement of pheochromocytoma in the venous phase; pheochromocytomas demonstrate venous phase attenuation values of up to 190 HU, whereas the maximum venous phase attenuation of ACA is 133 HU [69, 70]. Another crucial pitfall is the notion that all demonstrate marked hyperintensity on T2-weighted MRI (light bulb sign); in fact, pheochromocytomas can also present with isointensity or even hypointensity on T2-weighted images and therefore can possibly mimic other pathologies [71–73]. Careful imaging correlation to the clinical and biochemical testing is crucial for accurate diagnosis in the evaluation of a suspected pheochromocytoma.

Key points

- Up to one-third of pheochromocytomas demonstrate washout characteristics similar to ACA.
- Pheochromocytomas are vascular tumors and exhibit high attenuation, up to 190 HU, in the venous phase.
- Pheochromocytomas can present as iso- or hypointense on T2-weighted images, contrary to the notion that they always appear markedly hyperintense on T2-weighted images.

Small adrenocortical carcinoma

Adrenocortical carcinoma (ACC) is the most common primary malignant tumor involving the adrenal glands, with an estimated annual incidence of approximately 0.72 cases per million and accounting for 0.2% of all cancer-related deaths in the United States [74]. Approximately 30% of ACCs are incidentally seen on imaging [4]. ACC tends to be large (> 5 cm) at diagnosis and measures approximately 13 cm on average [75]. However, at least 9% of tumors are < 6 cm, and 3% are < 4 cm [76, 77]. These cases can be confused with adenomas because of their small size at diagnosis (Fig. 11). A case series has shown a number of ACCs that had a median size of 2.8 cm at diagnosis and were presumed benign, which led to delayed diagnosis and poor survival outcomes [78]. Adrenal CT protocol is helpful in this regard, as ACCs tend to demonstrate slow washout of contrast on delayed phases (< 40% at 15 min) [79].

Key points

- Three percent of ACCs are < 4 cm and can mimic ACAs on imaging based on their small size.
- ACCs typically demonstrate slow washout of contrast, with APW < 60%.

Mimics of adrenocortical carcinoma

Large adrenocortical adenoma

ACA is classically described as a small homogeneous adrenal nodule. ACAs have an average maximum dimension of 3 cm, whereas ACCs have an average maximum dimension of 6 cm. Although infrequent, ACAs can grow to be > 4 cm and occasionally even > 10 cm (Fig. 12) [80]. They can, rarely, demonstrate calcification, necrosis, and

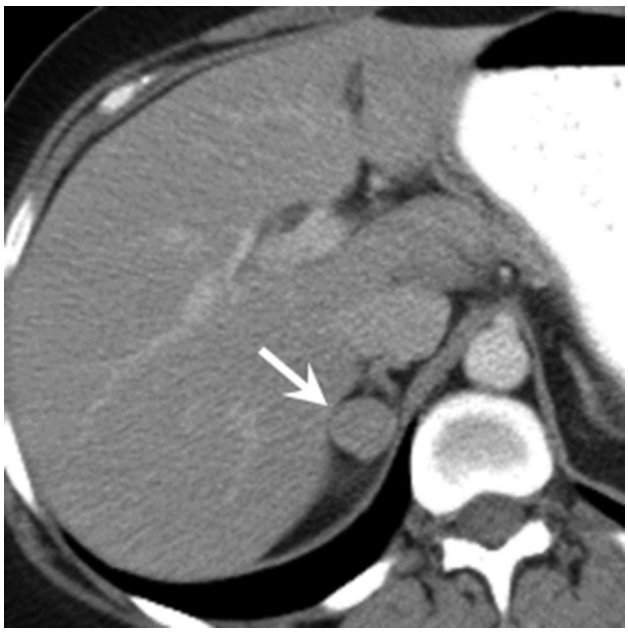

Fig. 11 An example of small adrenocortical carcinoma (ACC) mimicking an adrenal adenoma in a 43-year-old woman. Contrast-enhanced CT in the venous phase demonstrating a 1.5-cm nodule (arrow) within the right suprarenal region. This lesion was incidentally discovered on imaging and diagnosed as an adrenal adenoma based on size. It was followed up for a year and remained stable; however, follow-up CT, 2 years later, showed interval growth (not shown). The mass was surgically resected and pathological examination revealed an ACC

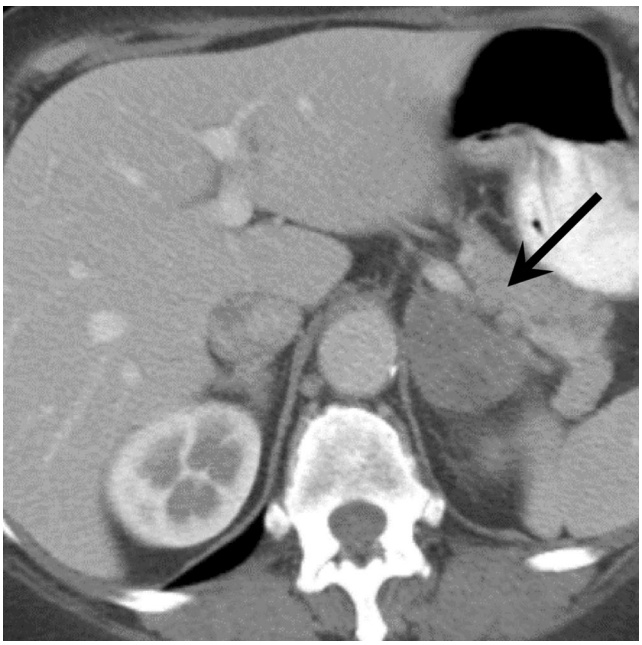

Fig. 12 An example of an adrenocortical adenoma mimicking an adrenocortical carcinoma in a 36-year-old man. Contrast-enhanced axial CT shows a well-circumscribed homogeneous mass (arrow) within the left adrenal gland with maximum axial dimension of 5.1 cm and attenuation of 58 HU on the venous phase. The mass was surgically resected and proven to be left adrenocortical adenoma despite being larger than 4 cm

hemorrhage, mimicking malignancy [81]. A diagnosis of ACA could be suspected in the presence of an unremarkable clinical presentation, stability over time, characteristic rapid washout patterns, lack of absolute features of malignancy such as invasion, and minimal FDG uptake on PET/CT. Nevertheless, surgical resection should be the standard of care for all adrenal masses measuring > 4 cm.

Key points

- ACA can grow in size > 4 cm and—rarely—can demonstrate calcifications, necrosis, and hemorrhage, mimicking ACC.
- ACA lacks the absolute features of malignancy such as invasion and metastases, and its stability over time can suggest diagnosis of a benign lesion.
- Surgical resection should remain the standard of care for large masses measuring > 4 cm.

Adrenal pseudocyst

Adrenal pseudocyst is the second most common cystic lesion involving the adrenal glands, constituting nearly 39% of all adrenal cysts [82]. Unlike true cysts, pseudocysts possess a fibrous capsule and lack a cellular lining; their etiology is unclear [83]. The majority of these cysts present with symptoms related to their large size are discovered incidentally on imaging [84]. The appearance of an adrenal pseudocyst on imaging can be similar to those of malignant lesions, especially ACC, because of the large size at diagnosis and the presence of intralesional hemorrhage, septations, and/or soft tissue component (Fig. 13). A thin, smooth wall enhancement can be frequently seen on MRI and CT [85]. Calcifications can also be seen in both adrenal pseudocysts and adrenal tumors. However, when compared with the central and irregular calcifications in adrenal tumors, pseudocysts tend to show more peripheral (mural) and regular curvilinear calcifications [55]. Intralesional hematomas appear as soft-tissue attenuation within the adrenal mass, mimicking ACC. Given the characteristic features of hematomas, attenuation values are variable on precontrast CT, depending on the age of the hematoma, and enhancement is typically absent in contrast-enhanced phases, although enhancement can be rarely encountered secondary to fibrosis [86].

Pseudocysts may also demonstrate low signal intensity on T1-weighted MRI sequences and high signal intensity on T2-weighted sequences. Due to their absence of metabolic activity, pseudocysts do not show FDG uptake on PET/CT, which is a helpful clue in differentiating an adrenal pseudocyst from ACC.

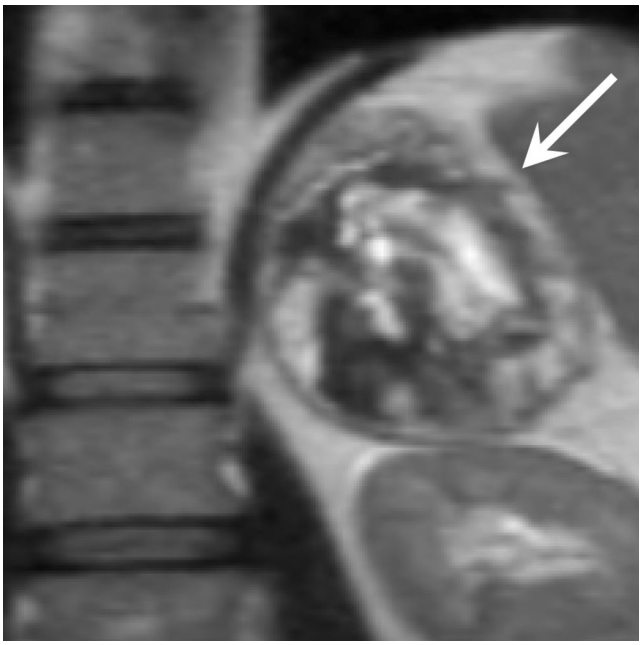

Fig. 13 An example of an adrenal pseudocyst mimicking an adrenocortical carcinoma in a 46-year-old man. T2-weighted coronal MRI shows a well-circumscribed large heterogeneous mass (arrow) within the left adrenal gland that was suspected to be an adrenocortical carcinoma. However, the mass was surgically resected and proven to be a left adrenal pseudocyst with intracystic hemorrhage

Key points

- Adrenal pseudocysts may contain calcifications that are typically peripheral and regular, compared with central and irregular calcifications in ACC.
- A thin, enhancing wall can be identified on contrast-enhanced studies.
- Postcontrast intralesional enhancement is not typically seen, although it can, rarely, be encountered due to fibrosis.
- Adrenal pseudocysts show no or minimal FDG uptake on PET/CT.

Ganglioneuroma

Ganglioneuroma is a rare benign tumor arising from neural crest tissue. Ganglioneuromas arising from the adrenal glands are uncommon and usually occur in patients younger than 20 years [87, 88]. Patients are typically asymptomatic, but some present with symptoms due to hormonal hypersecretion or abdominal/back pain attributed to mass effect by the tumor [89]. Adrenal ganglioneuroma is usually large at diagnosis, with a median maximum dimension of 8 cm. The classic CT appearance is a well-circumscribed mass with low attenuation on

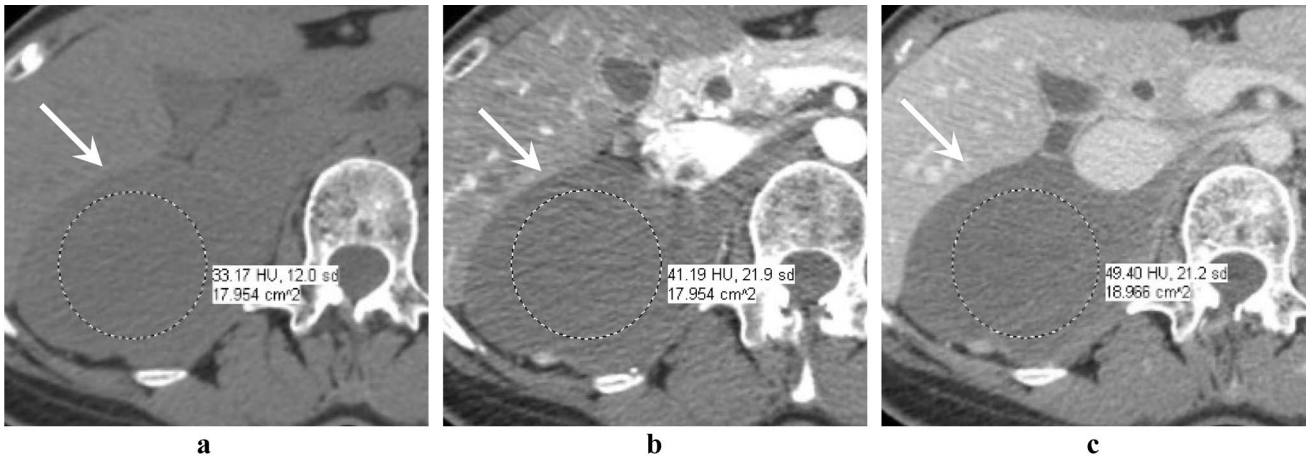

Fig. 14 An example of a surgically proven adrenal ganglioneuroma mimicking adrenocortical carcinoma in a 58-year-old woman. Contrast-enhanced axial CT shows a large homogeneous mass (arrow) in the right suprarenal region measuring 12.2 cm in maximal dimension with precontrast **a** attenuation of 33 HU, venous phase **b** attenuation of 41 HU, and delayed phase **c** attenuation of 49 HU showing progressive enhancement typical of adrenal ganglioneuroma

unenhanced images and progressive enhancement after intravenous contrast administration (Fig. 14) [89]. Familiarity with the typical imaging features of ganglioneuroma is crucial in distinguishing ganglioneuroma from ACC, as a ganglioneuroma could be mistaken for ACC because of its large size. MRI usually shows a homogeneous hypointense mass on T1-weighted images and a heterogeneous hyperintense mass on T2-weighted images.

Key points

– Ganglioneuroma is typically large at the time of diagnosis, mimicking ACC.
– The typical imaging features of ganglioneuroma are low attenuation and slight progressive enhancement after intravenous contrast administration.

ACC containing macroscopic fat mimicking myelolipoma

Although extremely rare, ACCs have been reported to contain bulk fat on imaging [90, 91]. The presence of macroscopic fat in an adrenal mass has been considered pathognomonic of an adrenal myelolipoma. However, adrenal tumors, including ACA and ACC, can undergo lipomatous metaplasia and therefore may demonstrate minor foci of bulk fat over time [92]. Fat-containing ACC is rarely encountered

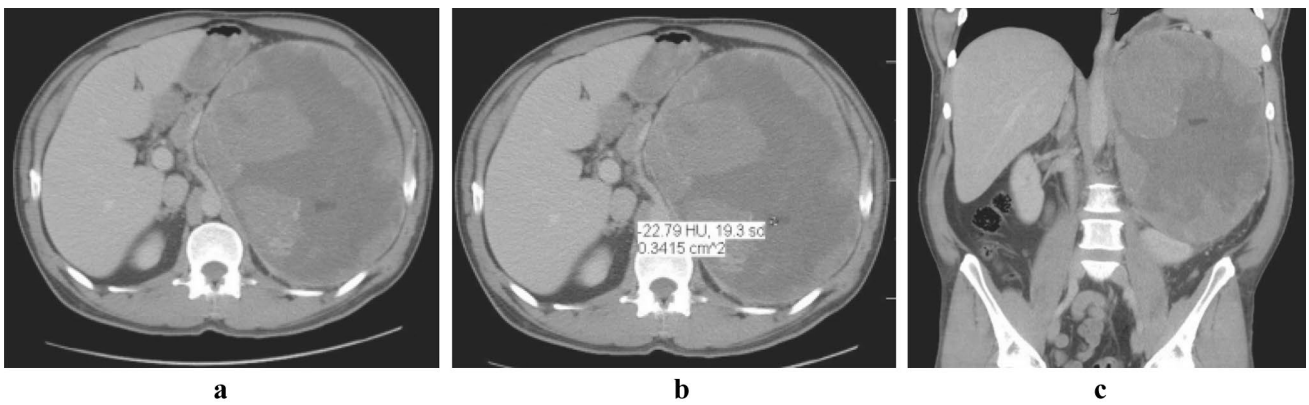

Fig. 15 An example of an adrenocortical carcinoma with bulk fat. Contrast-enhanced axial CT (**a**, **b**), and coronal reformatted (**c**), demonstrating a large heterogeneous mass with central necrosis and a small focus of fat attenuation (−23 HU) representative of bulk fat. Surgical resection confirmed the diagnosis of adrenocortical carcinoma with bulk fat. Reprinted with permission from BioMed Central (BMC). Egbert et al. [90]

and can be mistaken for an adrenal myelolipoma on imaging (Fig. 15).

An important clue to differentiate between both entities is the amount of fat present. Myelolipoma is known to contain major amount of fat, when compared to tumors undergoing lipomatous metaplasia containing minimal fat. Another clue depends on evaluation of prior imaging studies, when present. In fat-containing ACAs or ACCs, the development of the macroscopic fat foci can be seen over time.

Key points

- The presence of bulk fat within an adrenal mass is characteristic of adrenal myelolipoma.
- Bulk fat in ACC or ACA, when present, is minimal in amount.

Mimics of adrenal hyperplasia

Adrenocortical hyperplasia refers to the benign thickening of the adrenal glands on imaging; it is an unusual cause of hypercortisolism and hyperaldosteronism. Adrenocortical hyperplasia can be discovered incidentally without associated hormonal hypersecretion [93]. Imaging typically demonstrates diffuse thickening of the gland, which maintains its normal shape; less commonly, nodular enlargement can occur [26]. Bilateral multinodular appearance is typically seen in patients with ACTH-independent macronodular adrenal hyperplasia (Fig. 16); radiologists need to be familiar with this pattern to avoid misinterpreting adrenal hyperplasia as metastatic deposits. Some primary malignancies can secrete ACTH, leading to the development of ACTH-dependent adrenal hyperplasia, which can mimic metastases—especially in the context of underlying primary malignancy (Fig. 17).

Fig. 16 An example of ACTH-independent macronodular adrenal hyperplasia (AIMAH) mimicking metastases in a 42-year-old man. Contrast-enhanced axial CT shows bilateral multinodular enlargement of both adrenal glands (arrows), with more enlargement on the left side and CT attenuation ranging between 72 HU and 81 HU, compatible with bilateral adrenal metastases. Biochemical evaluation and surgical resection proved the mass to be AIMAH

Bilateral adrenal metastases and bilateral adrenal lymphoma

The adrenal gland is a relatively common location for metastatic disease [4]. Adrenal metastases are often bilateral and constitute an estimated 5.7% of bilateral adrenal lesions [94]. Adrenal metastases show inconsistent appearance on imaging; however, they can demonstrate bilateral diffuse or nodular thickening of the adrenal glands and maintain adreniform shape, resembling adrenocortical hyperplasia (Fig. 18). History of known malignancy is crucial in suggesting the possibility of metastatic deposits. Adrenal lymphoma, which rarely occurs, can appear identical to adrenal hyperplasia on imaging and is commonly bilateral [94, 95]. Given their interchangeable imaging appearance, adrenal lymphoma and metastatic lesions both can mimic adrenal hyperplasia and vice versa. Lymphoma and metastatic lesions both commonly exhibit low and moderate signal intensity on T1- and T2-weighted MRI, respectively, with progressive enhancement on contrast-enhanced T1 sequences. PET/CT is useful in such cases and usually shows intense FDG uptake; conversely, adrenal hyperplasia typically demonstrates FDG uptake that is just minimally increased above normal background [96].

Key points

- Bilateral adrenal metastases and lymphoma may manifest with adreniform thickening of the adrenal gland, mimicking adrenal hyperplasia.
- History of a primary malignancy highly suggests the possibility of adrenal metastases rather than adrenal hyperplasia.
- PET/CT can be useful, as it usually shows intense FDG uptake by metastases and lymphoma but not by hyperplasia.

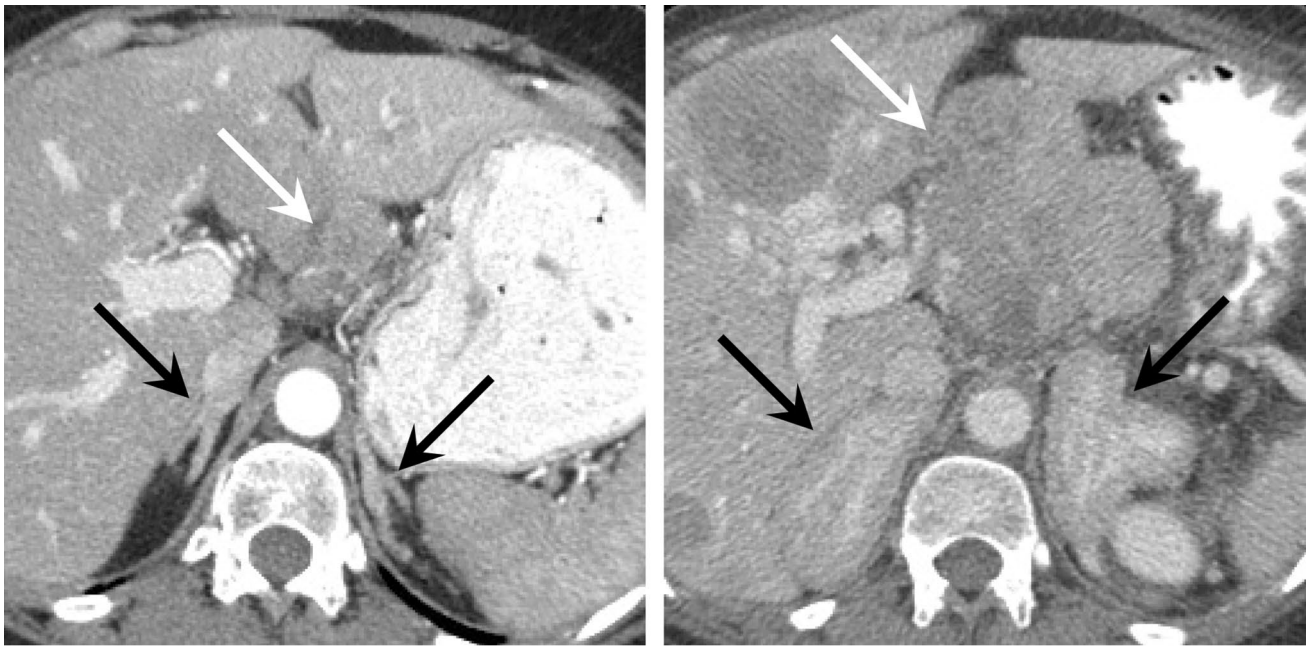

Fig. 17 An example of ACTH-dependent adrenal hyperplasia mimicking adrenal metastases in a 33-year-old woman with Cushing syndrome. Contrast-enhanced axial CT **a** shows diffusely enlarged adrenal glands (black arrows) secondary to ectopic ACTH production in the setting of a metastatic neuroendocrine tumor (NET) of the pancreas (white arrow). Follow-up contrast-enhanced axial CT at 9 months **b** shows progressive enlargement of the pancreatic NET (white arrow) with parallel enlargement of the adrenal glands. Thus, ACTH-dependent adrenal hyperplasia can mimic metastatic deposits due to the enlargement of the adrenal glands in the setting of an enlarging primary tumor

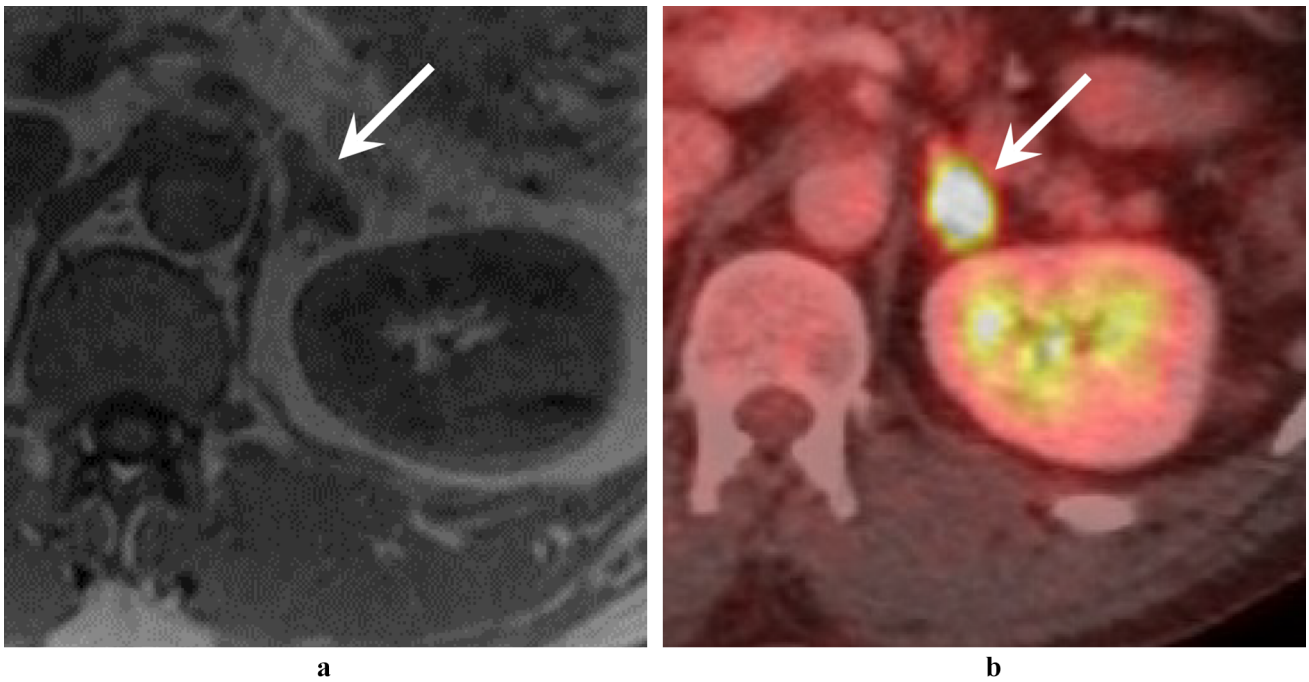

Fig. 18 An example of adrenal metastasis mimicking adrenal hyperplasia in a 56-year-old man with a history of metastatic melanoma. T1-weighted axial MRI **a** shows diffuse adreniform thickening of the left adrenal gland (arrow) appearing hypointense on T1, which is thought to represent adrenal hyperplasia. No abnormal diffusion restriction, enhancement, or T2 signal characteristics (not shown) within the left adrenal gland to suggest metastasis. However, PET/CT **b** shows avid FDG uptake (SUVmax = 18.9) in the left adrenal gland (arrow). The left adrenal gland was surgically resected and proven to have metastatic deposit from melanoma

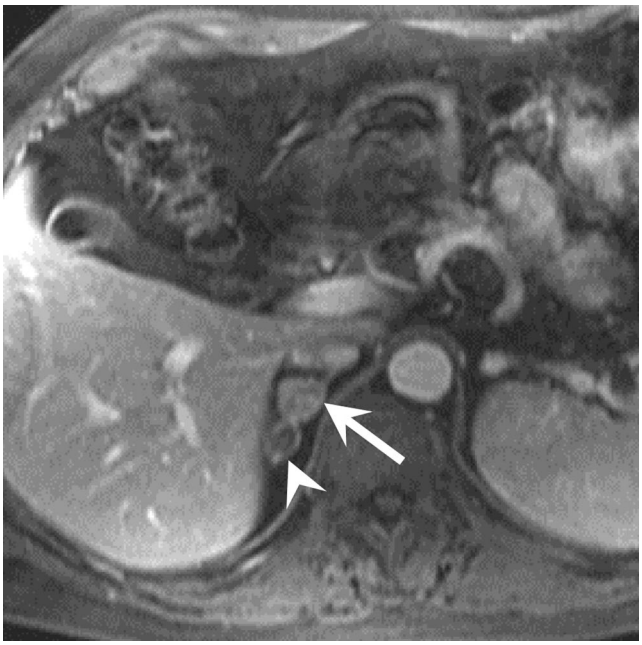

Fig. 19 An example of an adrenal collision tumor in a 59-year-old man with history of metastatic melanoma. T1-weighted contrast-enhanced axial MRI shows two distinct masses within the right adrenal gland; a 1.9 × 1.8 cm intracellular fat-containing adrenal adenoma (long arrow) that has been stable compared to prior imaging, showing signal drop on IP/OP (ASII = 38%). The other mass (arrowhead) is a 1.3 cm mildly enhancing adrenal nodule that has not been present on prior imaging, with no drop of signal on out-of-phase compared to in-phase pulse sequences (ASII = 7%). Pathological examination confirmed an adrenal collision tumor consisting of an adenoma and a metastasis

Adrenal collision tumor

A collision tumor is generally defined as a rare condition where two morphologically and pathologically distinct tumors, benign or malignant, co-exist in close proximity to each other within the same organ [97]. Collision tumors have been reported to involve a multitude of organs, including the liver, lungs, stomach, and adrenal glands [98, 99]. Collision tumors pose a diagnostic and therapeutic challenge because collision tumors consisting of a benign and malignant component can result in the malignant component going undiagnosed and possibly untreated. Therefore, accurate identification of these tumors is of utmost importance.

Adrenal collision tumors (ACTs) include a mixture of primary and secondary adrenal tumors and can mimic several adrenal pathologies on imaging (Fig. 19). Given the high prevalence of adenomas, they are the most commonly reported ACTs together with myelolipomas [100]. When an adrenal adenoma is present in an ACT, *heterogeneous* signal drop can be appreciated on OP compared with IP images [21]. Diagnosis of ACTs on imaging requires a high index of suspicion during evaluation of a heterogeneous adrenal mass. In addition, it is essential to correctly utilize different imaging modalities, as discussed before, to delineate the distinct tumor components based on their individual imaging features [100].

Key points

- Identification of collision tumors is essential for appropriate management.
- A new discernible nodule within a preexisting adrenal mass raises suspicion for ACT.

Conclusion

Pitfalls in adrenal imaging can be encountered due to several reasons; imaging technique-related pitfalls are common and include suboptimal delay during adrenal enhanced CT protocol. Adrenal pseudolesions represent another potential pitfall because of the close anatomical location of the adrenal glands to various abdominal organs. In addition, atypical features of certain pathologies and rare entities can have similar appearances to more common pathologies on imaging.

Compliance with ethical standards

Conflict of interest The authors declare that they have no disclosures.

References

1. Anagnostis P, Karagiannis A, Tziomalos K, Kakafika AI, Athyros VG, Mikhailidis DP (2009) Adrenal incidentaloma: a diagnostic challenge. Hormones (Athens, Greece) 8 (3):163-184
2. Barzon L, Sonino N, Fallo F, Palu G, Boscaro M (2003) Prevalence and natural history of adrenal incidentalomas. European journal of endocrinology 149 (4):273-285
3. Song JH, Chaudhry FS, Mayo-Smith WW (2008) The incidental adrenal mass on CT: prevalence of adrenal disease in 1,049 consecutive adrenal masses in patients with no known malignancy. AJR Am J Roentgenol 190 (5):1163-1168. https://doi.org/10.2214/ajr.07.2799
4. Tabarin A (2014) [Adrenal incidentalomas]. Presse medicale (Paris, France : 1983) 43 (4 Pt 1):393-400. https://doi.org/10.1016/j.lpm.2014.01.006
5. McCarthy CJ, McDermott S, Blake MA (2016) Adrenal Imaging: Magnetic Resonance Imaging and Computed Tomography. Frontiers of hormone research 45:55-69. https://doi.org/10.1159/000442313
6. Sangwaiya MJ, Boland GWL, Cronin CG, Blake MA, Halpern EF, Hahn PF (2010) Incidental Adrenal Lesions: Accuracy of Characterization with Contrast-enhanced Washout Multidetector

CT—10-minute Delayed Imaging Protocol Revisited in a Large Patient Cohort. Radiology 256 (2):504-510. https://doi.org/10.1148/radiol.10091386
7. Seo JM, Park BK, Park SY, Kim CK (2014) Characterization of lipid-poor adrenal adenoma: chemical-shift MRI and washout CT. AJR Am J Roentgenol 202 (5):1043-1050. https://doi.org/10.2214/ajr.13.11389
8. Caoili EM, Korobkin M, Francis IR, Cohan RH, Platt JF, Dunnick NR, Raghupathi KI (2002) Adrenal masses: characterization with combined unenhanced and delayed enhanced CT. Radiology 222 (3):629-633. https://doi.org/10.1148/radiol.2223010766
9. Caoili EM, Korobkin M, Francis IR, Cohan RH, Dunnick NR (2000) Delayed enhanced CT of lipid-poor adrenal adenomas. AJR Am J Roentgenol 175 (5):1411-1415. https://doi.org/10.2214/ajr.175.5.1751411
10. Pena CS, Boland GW, Hahn PF, Lee MJ, Mueller PR (2000) Characterization of indeterminate (lipid-poor) adrenal masses: use of washout characteristics at contrast-enhanced CT. Radiology 217 (3):798-802. https://doi.org/10.1148/radiology.217.3.r00dc29798
11. Korobkin M, Brodeur FJ, Francis IR, Quint L, Dunnick N, Londy F (1998) CT time-attenuation washout curves of adrenal adenomas and nonadenomas. AJR American journal of roentgenology 170 (3):747-752
12. Caoili EM, Korobkin M, Francis IR, Cohan RH, Dunnick NR (2000) Delayed Enhanced CT of Lipid-Poor Adrenal Adenomas. American Journal of Roentgenology 175 (5):1411-1415. https://doi.org/10.2214/ajr.175.5.1751411
13. Blake MA, Kalra MK, Sweeney AT, Lucey BC, Maher MM, Sahani DV, Halpern EF, Mueller PR, Hahn PF, Boland GW (2006) Distinguishing benign from malignant adrenal masses: multi-detector row CT protocol with 10-minute delay. Radiology 238 (2):578-585. https://doi.org/10.1148/radiol.2382041514
14. Ng CS, Altinmakas E, Wei W, Ghosh P, Li X, Grubbs EG, Perrier ND, Lee JE, Prieto VG, Hobbs BP (2018) Utility of Intermediate-Delay Washout CT Images for Differentiation of Malignant and Benign Adrenal Lesions: A Multivariate Analysis. American Journal of Roentgenology 211 (2):W109-W115. https://doi.org/10.2214/ajr.17.19103
15. Lee JM, Kim MK, Ko SH, Koh JM, Kim BY, Kim SW, Kim SK, Kim HJ, Ryu OH, Park J, Lim JS, Kim SY, Shong YK, Yoo SJ, Korean Endocrine Society CfCPG (2017) Clinical Guidelines for the Management of Adrenal Incidentaloma. Endocrinology and metabolism (Seoul, Korea) 32 (2):200-218. https://doi.org/10.3803/enm.2017.32.2.200
16. Mayo-Smith WW, Song JH, Boland GL, Francis IR, Israel GM, Mazzaglia PJ, Berland LL, Pandharipande PV (2017) Management of Incidental Adrenal Masses: A White Paper of the ACR Incidental Findings Committee. Journal of the American College of Radiology 14 (8):1038-1044. https://doi.org/10.1016/j.jacr.2017.05.001
17. Boland GW, Lee MJ, Gazelle GS, Halpern EF, McNicholas MM, Mueller PR (1998) Characterization of adrenal masses using unenhanced CT: an analysis of the CT literature. AJR Am J Roentgenol 171 (1):201-204. https://doi.org/10.2214/ajr.171.1.9648789
18. Hamrahian AH, Ioachimescu AG, Remer EM, Motta-Ramirez G, Bogabathina H, Levin HS, Reddy S, Gill IS, Siperstein A, Bravo EL (2005) Clinical Utility of Noncontrast Computed Tomography Attenuation Value (Hounsfield Units) to Differentiate Adrenal Adenomas/Hyperplasias from Nonadenomas: Cleveland Clinic Experience. The Journal of Clinical Endocrinology & Metabolism 90 (2):871-877. https://doi.org/10.1210/jc.2004-1627
19. Becker-Weidman D, Kalb B, Mittal PK, Harri PA, Arif-Tiwari H, Farris AB, Chen Z, Sungjin K, Martin DR (2015) Differentiation of lipid-poor adrenal adenomas from non-adenomas with magnetic resonance imaging: Utility of dynamic, contrast enhancement and single-shot T2-weighted sequences. European Journal of Radiology 84 (11):2045-2051. doi:https://doi.org/10.1016/j.ejrad.2015.06.032
20. Mitchell DG, Crovello M, Matteucci T, Petersen RO, Miettinen MM (1992) Benign adrenocortical masses: diagnosis with chemical shift MR imaging. Radiology 185 (2):345-351. https://doi.org/10.1148/radiology.185.2.1410337
21. Adam SZ, Nikolaidis P, Horowitz JM, Gabriel H, Hammond NA, Patel T, Yaghmai V, Miller FH (2016) Chemical Shift MR Imaging of the Adrenal Gland: Principles, Pitfalls, and Applications. RadioGraphics 36 (2):414-432. https://doi.org/10.1148/rg.2016150139
22. Haider MA, Ghai S, Jhaveri K, Lockwood G (2004) Chemical shift MR imaging of hyperattenuating (>10 HU) adrenal masses: does it still have a role? Radiology 231 (3):711-716. https://doi.org/10.1148/radiol.2313030676
23. Davarpanah AH, Israel GM (2014) MR Imaging of the Kidneys and Adrenal Glands. Radiologic clinics of North America 52 (4):779-798. doi:https://doi.org/10.1016/j.rcl.2014.02.003
24. Schieda N, Al Dandan O, Kielar AZ, Flood TA, McInnes MDF, Siegelman ES (2014) Pitfalls of adrenal imaging with chemical shift MRI. Clinical Radiology 69 (11):1186-1197. doi:https://doi.org/10.1016/j.crad.2014.06.020
25. Israel GM, Korobkin M, Wang C, Hecht EN, Krinsky GA (2004) Comparison of unenhanced CT and chemical shift MRI in evaluating lipid-rich adrenal adenomas. AJR Am J Roentgenol 183 (1):215-219. https://doi.org/10.2214/ajr.183.1.1830215
26. Blake MA, Cronin CG, Boland GW (2010) Adrenal imaging. AJR Am J Roentgenol 194 (6):1450-1460. https://doi.org/10.2214/ajr.10.4547
27. Karstaedt N, Sagel SS, Stanley RJ, Melson GL, Levitt RG (1978) Computed tomography of the adrenal gland. Radiology 129 (3):723-730. https://doi.org/10.1148/129.3.723
28. Gokan T, Ohgiya Y, Nobusawa H, Munechika H (2005) Commonly encountered adrenal pseudotumours on CT. The British journal of radiology 78 (926):170-174. https://doi.org/10.1259/bjr/18362306
29. Chasse E, Buggenhout A, Zalcman M, Jeanmart J, Gelin M, El Nakadi I (2003) Gastric diverticulum simulating a left adrenal tumor. Surgery 133 (4):447-448. doi:https://doi.org/10.1067/msy.2003.47
30. Anaise D, Brand DL, Smith NL, Soroff HS (1984) Pitfalls in the diagnosis and treatment of a symptomatic gastric diverticulum. Gastrointestinal Endoscopy 30 (1):28-30. doi:https://doi.org/10.1016/S0016-5107(84)72291-7
31. Meeroff M, Gollan JR, Meeroff JC (1967) Gastric diverticulum. The American journal of gastroenterology 47 (3):189-203
32. Noguera JJ, Benito A, Hernandez-Sastre C, Cano D, Vivas I, Gonzalez-Crespo I (2009) Gastric Diverticulum Mimicking Cystic Lesion in Left Adrenal Gland. Urology 73 (5):997-998. doi:https://doi.org/10.1016/j.urology.2008.11.019
33. Chung SD, Shih-chieh Chueh J, Yu HJ (2012) Laparoscopic resection of gastric gastrointestinal stromal tumors presenting as left adrenal tumors. World Journal of Gastroenterology 18 (1):96-98. https://doi.org/10.3748/wjg.v18.i1.96
34. Kim HJ, Lee DH, Lim JW, Ko YT, Kim KW (2008) Exophytic benign and malignant hepatic tumors: CT imaging features. Korean journal of radiology 9 (1):67-75. https://doi.org/10.3348/kjr.2008.9.1.67
35. Dong A, Zhong X, Wang Y (2018) Pedunculated Hepatocellular Carcinoma Mimicking Right Adrenal Tumor on FDG PET/CT. Clinical nuclear medicine 43 (7):e242-e244. https://doi.org/10.1097/rlu.0000000000002096

36. Tran-Minh VA, Gindre T, Pracros JP, Morin de Finfe CH, Kattan M, Peix JL (1991) Volvulus of a pedunculated hemangioma of the liver. American Journal of Roentgenology 156 (4):866-867. https://doi.org/10.2214/ajr.156.4.2003458
37. Brancatelli G, Federle MP, Blachar A, Grazioli L (2001) Hemangioma in the cirrhotic liver: diagnosis and natural history. Radiology 219 (1):69-74. https://doi.org/10.1148/radiology.219.1.r01ap3269
38. Sabri SS, Saad WEA (2011) Anatomy and Classification of Gastrorenal and Gastrocaval Shunts. Seminars in Interventional Radiology 28 (3):296-302. https://doi.org/10.1055/s-0031-1284456
39. Loukas M, Louis RG, Jr., Hullett J, Loiacano M, Skidd P, Wagner T (2005) An anatomical classification of the variations of the inferior phrenic vein. Surgical and radiologic anatomy: SRA 27 (6):566-574. https://doi.org/10.1007/s00276-005-0029-0
40. Mitty HA, Cohen BA, Sprayregen S, Schwartz K (1983) Adrenal pseudotumors on CT due to dilated portosystemic veins. American Journal of Roentgenology 141 (4):727-730. https://doi.org/10.2214/ajr.141.4.727
41. Masand P (2014) Radiographic findings associated with vascular anomalies. Seminars in plastic surgery 28 (2):69-78. https://doi.org/10.1055/s-0034-1376266
42. Sleightholm R, Wahlmeier S, Carson JS, Drincic A, Lazenby A, Foster JM (2016) Massive adrenal vein aneurysm mimicking an adrenal tumor in a patient with hemophilia A: a case report and review of the literature. Journal of medical case reports 10 (1):343. https://doi.org/10.1186/s13256-016-1108-z
43. Mortele KJ, Mortele B, Silverman SG (2004) CT features of the accessory spleen. AJR American journal of roentgenology 183 (6):1653-1657. https://doi.org/10.2214/ajr.183.6.01831653
44. Gayer G, Zissin R, Apter S, Atar E, Portnoy O, Itzchak Y (2001) CT findings in congenital anomalies of the spleen. The British journal of radiology 74 (884):767-772. https://doi.org/10.1259/bjr.74.884.740767
45. Chen C-H, Wu H-C, Chang C-H (2005) An accessory spleen mimics a left adrenal carcinoma. MedGenMed: Medscape general medicine 7 (2):9-9
46. Perez Melon C, Esteban Morcillo J, Salgado C, Castro Bande M, Armada Rodriguez E, Otero Gonzalez A (1998) Incidentaloma due to abdominal splenosis. Nephron 80 (3):359-360. https://doi.org/10.1159/000045202
47. Hagan I, Hopkins R, Lyburn I (2006) Superior demonstration of splenosis by heat-denatured Tc-99 m red blood cell scintigraphy compared with Tc-99 m sulfur colloid scintigraphy. Clinical nuclear medicine 31 (8):463-466. https://doi.org/10.1097/01.rlu.0000226907.36840.b3
48. Bybel B, Brunken RC, DiFilippo FP, Neumann DR, Wu G, Cerqueira MD (2008) SPECT/CT imaging: clinical utility of an emerging technology. Radiographics 28 (4):1097-1113. https://doi.org/10.1148/rg.284075203
49. Ward EM, Rorie DK, Nauss LA, Bahn RC (1979) The celiac ganglia in man: normal anatomic variations. Anesthesia and analgesia 58 (6):461-465
50. Wang ZJ, Webb EM, Westphalen AC, Coakley FV, Yeh BM (2010) Multi-detector row computed tomographic appearance of celiac ganglia. Journal of computer assisted tomography 34 (3):343-347. https://doi.org/10.1097/rct.0b013e3181d26ddd
51. Dal Pozzo G, Bozza A, Fargnoli R, Brizzi E (1985) CT identification of coeliac ganglia. Eur J Radiol 5 (1):24-26
52. Castro L, Schutte H, Richardson C, Fernandez RR, Newman HR (1975) Adrenal cyst. Urology 5 (4):574-577
53. Khoda J, Hertzanu Y, Sebbag G, Lantsberg L, Barky Y (1993) Adrenal cysts: diagnosis and therapeutic approach. International surgery 78 (3):239-242
54. Johnson PT, Horton KM, Fishman EK (2009) Adrenal imaging with MDCT: Nonneoplastic disease. AJR Am J Roentgenol 193 (4):1128-1135. https://doi.org/10.2214/ajr.09.2551
55. Rozenblit A, Morehouse HT, Amis ES, Jr. (1996) Cystic adrenal lesions: CT features. Radiology 201 (2):541-548. https://doi.org/10.1148/radiology.201.2.8888255
56. Abrams HL, Spiro R, Goldstein N (1950) Metastases in carcinoma. Analysis of 1000 autopsied cases. Cancer 3 (1):74-85. doi:https://doi.org/10.1002/1097-0142(1950)3:1%3c74::aid-cncr2820030111%3e3.0.co;2-7
57. Arnold DT, Reed JB, Burt K (2003) Evaluation and management of the incidental adrenal mass. Proceedings (Baylor University Medical Center) 16 (1):7-12
58. Choi YA, Kim CK, Park BK, Kim B (2013) Evaluation of adrenal metastases from renal cell carcinoma and hepatocellular carcinoma: use of delayed contrast-enhanced CT. Radiology 266 (2):514-520. https://doi.org/10.1148/radiol.12120110
59. Woo S, Cho JY, Kim SY, Kim SH (2014) Adrenal adenoma and metastasis from clear cell renal cell carcinoma: can they be differentiated using standard MR techniques? Acta radiologica (Stockholm, Sweden: 1987) 55 (9):1120-1128. https://doi.org/10.1177/0284185113512301
60. Elsayes KM, Emad-Eldin S, Morani AC, Jensen CT (2017) Practical Approach to Adrenal Imaging. Radiol Clin North Am 55 (2):279-301. https://doi.org/10.1016/j.rcl.2016.10.005
61. Metser U, Miller E, Lerman H, Lievshitz G, Avital S, Even-Sapir E (2006) 18F-FDG PET/CT in the evaluation of adrenal masses. Journal of nuclear medicine: official publication, Society of Nuclear Medicine 47 (1):32-37
62. Lenders JWM, Eisenhofer G, Mannelli M, Pacak K (2005) Phaeochromocytoma. The Lancet 366 (9486):665-675. doi:https://doi.org/10.1016/S0140-6736(05)67139-5
63. Motta-Ramirez GA, Remer EM, Herts BR, Gill IS, Hamrahian AH (2005) Comparison of CT Findings in Symptomatic and Incidentally Discovered Pheochromocytomas. American Journal of Roentgenology 185 (3):684-688. https://doi.org/10.2214/ajr.185.3.01850684
64. Shen WT, Sturgeon C, Clark OH, Duh Q-Y, Kebebew E (2004) Should pheochromocytoma size influence surgical approach? A comparison of 90 malignant and 60 benign pheochromocytomas. Surgery 136 (6):1129-1137. https://doi.org/10.1016/j.surg.2004.05.058
65. Saginoya T, Miyake H, Kiyosue H, Okahara M, Hori Y, Hata H, Mori H (2001) [Significance of CT findings and catecholamine determination in peripheral blood of asymptomatic pheochromocytoma and paraganglioma]. Nihon Igaku Hoshasen Gakkai zasshi Nippon acta radiologica 61 (1):33-38
66. Park BK, Kim B, Ko K, Jeong SY, Kwon GY (2006) Adrenal masses falsely diagnosed as adenomas on unenhanced and delayed contrast-enhanced computed tomography: pathological correlation. Eur Radiol 16 (3):642-647. https://doi.org/10.1007/s00330-005-0017-0
67. Park BK, Kim CK, Kwon GY, Kim JH (2007) Re-evaluation of pheochromocytomas on delayed contrast-enhanced CT: washout enhancement and other imaging features. Eur Radiol 17 (11):2804-2809. https://doi.org/10.1007/s00330-007-0695-x
68. Patel J, Davenport MS, Cohan RH, Caoili EM (2013) Can established CT attenuation and washout criteria for adrenal adenoma accurately exclude pheochromocytoma? AJR Am J Roentgenol 201 (1):122-127. https://doi.org/10.2214/ajr.12.9620
69. Blake MA, Krishnamoorthy SK, Boland GW, Sweeney AT, Pitman MB, Harisinghani M, Mueller PR, Hahn PF (2003) Low-density pheochromocytoma on CT: a mimicker of adrenal adenoma. AJR Am J Roentgenol 181 (6):1663-1668. https://doi.org/10.2214/ajr.181.6.1811663

70. Northcutt BG, Raman SP, Long C, Oshmyansky AR, Siegelman SS, Fishman EK, Johnson PT (2013) MDCT of adrenal masses: Can dual-phase enhancement patterns be used to differentiate adenoma and pheochromocytoma? AJR Am J Roentgenol 201 (4):834-839. https://doi.org/10.2214/ajr.12.9753
71. Fonseca EKUN, Ponte MPTR, Yamauchi FI, Baroni RH (2017) The light bulb sign in pheochromocytoma. Abdominal Radiology 42 (11):2779-2779. https://doi.org/10.1007/s00261-017-1198-0
72. Varghese JC, Hahn PF, Papanicolaou N, Mayo-Smith WW, Gaa JA, Lee MJ (1997) MR differentiation of phaeochromocytoma from other adrenal lesions based on qualitative analysis of T2 relaxation times. Clin Radiol 52 (8):603-606
73. McDermott S, McCarthy CJ, Blake MA (2015) Images of pheochromocytoma in adrenal glands. Gland Surgery 4 (4):350-358. https://doi.org/10.3978/j.issn.2227-684x.2014.11.06
74. Kebebew E, Reiff E, Duh QY, Clark OH, McMillan A (2006) Extent of disease at presentation and outcome for adrenocortical carcinoma: have we made progress? World journal of surgery 30 (5):872-878. https://doi.org/10.1007/s00268-005-0329-x
75. Bharwani N, Rockall AG, Sahdev A, Gueorguiev M, Drake W, Grossman AB, Reznek RH (2011) Adrenocortical carcinoma: the range of appearances on CT and MRI. AJR Am J Roentgenol 196 (6):W706-714. https://doi.org/10.2214/ajr.10.5540
76. Sturgeon C, Shen WT, Clark OH, Duh QY, Kebebew E (2006) Risk assessment in 457 adrenal cortical carcinomas: how much does tumor size predict the likelihood of malignancy? Journal of the American College of Surgeons 202 (3):423-430. https://doi.org/10.1016/j.jamcollsurg.2005.11.005
77. Paton BL, Novitsky YW, Zerey M, Harrell AG, Norton HJ, Asbun H, Kercher KW, Heniford BT (2006) Outcomes of adrenal cortical carcinoma in the United States. Surgery 140 (6):914-920; discussion 919-920. https://doi.org/10.1016/j.surg.2006.07.035
78. Ozsari L, Kutahyalioglu M, Elsayes KM, Vicens RA, Sircar K, Jazaerly T, Waguespack SG, Busaidy NL, Cabanillas ME, Dadu R, Hu MI, Vassilopoulou-Sellin R, Jimenez C, Lee JE, Habra MA (2016) Preexisting adrenal masses in patients with adrenocortical carcinoma: clinical and radiological factors contributing to delayed diagnosis. Endocrine 51 (2):351-359. https://doi.org/10.1007/s12020-015-0694-7
79. Willatt J, Chong S, Ruma JA, Kuriakose J (2015) Incidental Adrenal Nodules and Masses: The Imaging Approach. International Journal of Endocrinology 2015:410185. https://doi.org/10.1155/2015/410185
80. Barnett CC, Jr., Varma DG, El-Naggar AK, Dackiw AP, Porter GA, Pearson AS, Kudelka AP, Gagel RF, Evans DB, Lee JE (2000) Limitations of size as a criterion in the evaluation of adrenal tumors. Surgery 128 (6):973-982;discussion 982-973. https://doi.org/10.1067/msy.2000.110237
81. Newhouse JH, Heffess CS, Wagner BJ, Imray TJ, Adair CF, Davidson AJ (1999) Large degenerated adrenal adenomas: radiologic-pathologic correlation. Radiology 210 (2):385-391. https://doi.org/10.1148/radiology.210.2.r99fe12385
82. Erickson LA, Lloyd RV, Hartman R, Thompson G (2004) Cystic adrenal neoplasms. Cancer 101 (7):1537-1544. https://doi.org/10.1002/cncr.20555
83. Groben PA, Roberson JB, Jr., Anger SR, Askin FB, Price WG, Siegal GP (1986) Immunohistochemical evidence for the vascular origin of primary adrenal pseudocysts. Archives of pathology & laboratory medicine 110 (2):121-123
84. Mansmann G, Lau J, Balk E, Rothberg M, Miyachi Y, Bornstein SR (2004) The clinically inapparent adrenal mass: update in diagnosis and management. Endocrine reviews 25 (2):309-340. https://doi.org/10.1210/er.2002-0031
85. Ricci Z, Chernyak V, Hsu K, Mazzariol FS, Flusberg M, Oh S, Stein M, Rozenblit A (2013) Adrenal cysts: Natural history by long-term imaging follow-up. American Journal of Roentgenology 201 (5):1009-1016. https://doi.org/10.2214/ajr.12.9202
86. Wang LJ, Wong YC, Chen CJ, Chu SH (2003) Imaging spectrum of adrenal pseudocysts on CT. European radiology 13 (3):531-535. https://doi.org/10.1007/s00330-002-1537-5
87. Geoerger B, Hero B, Harms D, Grebe J, Scheidhauer K, Berthold F (2001) Metabolic activity and clinical features of primary ganglioneuromas. Cancer 91 (10):1905-1913
88. Carrion Lopez P, Martinez Ruiz J, Martinez Sanchiz C, Peran Teruel M, Atienzar Tobarra M, Donate Moreno MJ, Virseda Rodriguez JA (2012) Adrenal ganglioneuroma. Archivos espanoles de urologia 65 (8):773-776
89. Hassan S, M. EK, Sanaz J, Ajaykumar M, D. WM, E. LJ, G. WS, L. BN, Rena VS, Camilo J, Amir HM (2014) Adrenal ganglioneuroma: features and outcomes of 27 cases at a referral cancer centre. Clinical endocrinology 80 (3):342-347. doi:https://doi.org/10.1111/cen.12320
90. Egbert N, Elsayes KM, Azar S, Caoili EM (2010) Computed tomography of adrenocortical carcinoma containing macroscopic fat. Cancer imaging: the official publication of the International Cancer Imaging Society 10 (1):198-200. https://doi.org/10.1102/1470-7330.2010.0029
91. Montone K, Rosen M, Siegelman E, Fogt F, LiVolsi V (2009) Adrenocortical neoplasms with myelolipomatous and lipomatous metaplasia: report of 3 cases. Endocrine Practice 15 (2):128-133
92. Taner AT, Schieda N, Siegelman ES (2015) Pitfalls in Adrenal Imaging. Seminars in Roentgenology 50 (4):260-272. doi:https://doi.org/10.1053/j.ro.2015.08.002
93. Li L-l, Gu W-j, Dou J-t, Yang G-q, Lv Z-h, Mu Y-m, Lu J-m (2015) Incidental Adrenal Enlargement: An Overview from a Retrospective Study in a Chinese Population. International Journal of Endocrinology 2015:192874. https://doi.org/10.1155/2015/192874
94. Lomte N, Bandgar T, Khare S, Jadhav S, Lila A, Goroshi M, Kasaliwal R, Khadilkar K, Shah NS (2016) Bilateral adrenal masses: a single-centre experience. Endocrine Connections 5 (2):92-100. https://doi.org/10.1530/ec-16-0015
95. Rashidi A, Fisher SI (2013) Primary adrenal lymphoma: a systematic review. Annals of hematology 92 (12):1583-1593. https://doi.org/10.1007/s00277-013-1812-3
96. Mayo-Smith WW, Boland GW, Noto RB, Lee MJ (2001) State-of-the-art adrenal imaging. Radiographics: a review publication of the Radiological Society of North America, Inc 21 (4):995-1012. https://doi.org/10.1148/radiographics.21.4.g01jl21995
97. Sung CT, Shetty A, Menias CO, Houshyar R, Chatterjee S, Lee TK, Tung P, Helmy M, Lall C (2017) Collision and composite tumors; radiologic and pathologic correlation. Abdominal radiology (New York) 42 (12):2909-2926. https://doi.org/10.1007/s00261-017-1200-x
98. Donahue S, Gollapudi A (2018) PRIMARY PULMONARY COLLISION TUMOR WITH ADENOCARCINOMA AND SCLC. CHEST 154 (4):601A. https://doi.org/10.1016/j.chest.2018.08.542
99. Michalinos A, Constantinidou A, Kontos M (2015) Gastric Collision Tumors: An Insight into Their Origin and Clinical Significance. Gastroenterology Research and Practice 2015:8. https://doi.org/10.1155/2015/314158

100. Katabathina VS, Flaherty E, Kaza R, Ojili V, Chintapalli KN, Prasad SR (2013) Adrenal collision tumors and their mimics: multimodality imaging findings. Cancer imaging: the official publication of the International Cancer Imaging Society 13 (4):602-610. https://doi.org/10.1102/1470-7330.2013.0053